Journal of Photochemistry and Photobiology A: Chemistry 217 (2011) 363–368

Contents lists available at ScienceDirect

Journal of Photochemistry and Photobiology A: Chemistry

journal homepage: www.elsevier.com/locate/jphotochem

The early processes in the photochemistry of *ortho*-nitrobenzyl acetate

T. Schmierer[a,b], F. Bley[c], K. Schaper[c], P. Gilch[a,b,*]

[a] Fakultät für Physik, Ludwig-Maximilians-Universität, Oettingenstr. 67, D-80538 München, Germany
[b] Institut für Physikalische Chemie, Heinrich-Heine-Universität Düsseldorf, Universitätstr. 1, D-40225 Düsseldorf, Germany
[c] Institut für Organische Chemie und Makromolekulare Chemie, Heinrich-Heine-Universität Düsseldorf, Universitätstr. 1, D-40225 Düsseldorf, Germany

ARTICLE INFO

Article history:
Received 17 September 2010
Received in revised form 3 November 2010
Accepted 8 November 2010
Available online 18 November 2010

Keywords:
Femtosecond spectroscopy
Photo-labile protecting groups
Nitro arenes
Hydrogen transfer

ABSTRACT

The early processes in the de-caging of acetic acid from o-nitrobenzyl acetate (oNBAc) were studied by femtosecond techniques. Solutions of oNBAc in acetonitrile were excited by 260 nm laser pulses and the resulting spectroscopic changes probed by transient absorption and stimulated Raman spectroscopy. Absorption and Raman data give evidence of the formation of an *aci*-nitro species resulting from an intramolecular hydrogen transfer. The species is formed on the 1 ps and 1 ns time scale in equal amounts. The two processes are attributed to hydrogen transfers via a singlet and a triplet channel. The overall quantum yield of the *aci*-nitro formation is 0.1 matching the de-caging yield.

1. Introduction

Already in the 1960s the *ortho*-nitrobenzyl moiety was introduced as a photolabile protecting group [1–4]. In the 1970s the concept of caged compounds was introduced based on their photoreaction [5,6]. Caged compounds find applications in biophysical investigations [7,8] and in the in-situ synthesis of DNA chips [9–11]. Many improvements regarding the photochemical properties, especially concerning the quantum yield, of caged compounds have been made either by modification of the *ortho*-nitrobenzyl moiety [12,13], by using other caging groups [14] or by sensitized irradiation [15]. Quite a few types of caging groups are available today, but the *ortho*-nitrobenzyl moiety and its derivatives are most frequently used. Consequently, they have been subject to numerous kinetic studies [16–18] aiming at the mechanism of the photo-release and eventually an improved performance. Consensus has been reached that the photo-release involves a cascade of elementary processes evolving on various time scales. It is commonly assumed [4] that primarily a hydrogen transfer from the *ortho*-substituent to the nitro group occurs. The transfer results in the formation of an *aci*-nitro tautomer. For several molecules bearing the nitrobenzyl and related residues the fate of the *aci*-nitro forms has been studied by laser flash photolysis [18] and step-scan FTIR [16,17]. Concerning the formation of the *aci*-nitro form a series of papers were published in the 1980s and 1990s by Yip et al. [19–22]. In picosecond pump probe experiments they observed an absorption band around 400 nm – a spectral region where *aci*-nitro forms are known to absorb [23]. They reported a (partial) rise of these bands within their instrumental response time (~40 ps) and thus could only report an upper boundary for the formation time of the *aci*-nitro tautomers. Further, triplet states of nitrobenzene derivatives also feature a band around 400 nm [19] hampering the spectroscopic identification of *aci*-nitro tautomers on the picosecond time scale.

In previous reports on the photochemistry of *ortho*-nitrobenzaldehyde [24,25] and the (reversible) photo-tautomerisation of *ortho*-nitrotoluene (oNT) [26] we have shown that the respective *aci*-nitro forms exhibit highly characteristic Raman spectra ideally suited to trace their formation. Here, we will employ this spectroscopic marker to investigate the early (up to some nanoseconds) processes in deprotection. For the study we have chosen *ortho*-nitrobenzyl acetate (oNBAc). The structural similarity between oNT and the *ortho*-nitrobenzyl moiety will allow a direct comparison between the published data on the reversible tautomerisation of the former and the irreversible of the latter. The acetate represents leaving groups containing the carboxylate function often subject to photo-protection. In the remainder of the paper we will first describe femtosecond transient absorption data on oNBAc. These data deliver information on time constants and yields for the early processes and on the electronic states involved. The identification of the *aci*-nitro-tautomer will rest on femtosecond stimulated Raman spectroscopy (FSRS) [27]. In all experiments reported in the

* Corresponding author at: Institut für Physikalische Chemie, Heinrich-Heine-Universität Düsseldorf, Universitätstr. 1, D-40225 Düsseldorf, Germany.
Tel.: +49 211 81 15400; fax: +49 211 81 12803.
E-mail address: Peter.Gilch@uni-duesseldorf.de (P. Gilch).

1010-6030/$ – see front matter © 2010 Elsevier B.V. All rights reserved.
doi:10.1016/j.jphotochem.2010.11.006

following acetonitrile (perdeuterated in FSRS) served as a solvent. Perdeuterated acetonitrile is poor of vibrational resonances in the spectral range of interest rendering it a solvent of choice for the FSRS measurements. Further, we will compare laser flash experiments on oNBAc [18] with the transient absorption data reported here. The flash experiments have been performed using acetonitrile as a solvent.

2. Experimental methods

The experimental set-ups for the transient absorption (TA) and FSRS experiments have been detailed before [25,28]. The pertinent parameters and procedures for the pump probe data acquisition are briefly summarized in the following. Actinic pump pulses at 258 nm were obtained by frequency tripling of a portion of the output of a Clark CPA 2001 laser amplifier system (1 kHz). The energy of these pulses amounted to 300 nJ (TA) and 500 nJ (FSRS). Actinic pump beams were focused onto the sample to arrive at diameters of 80 μm (TA) and 40 μm (FSRS). White light pulses generated in a CaF_2 plate served as probe light for TA and FSRS. The respective diameters at the sample locations were 40 μm (TA) and 20 μm (FSRS). After passing the sample the probe light was directed to a grating spectrograph and detected with a diode array. In the TA experiment the covered spectral range (310–750 nm) is larger than one octave. Therefore, the detection of UV light diffracted in second order had to be suppressed. This was achieved by placing UV blocking filters in front of the "red part" of the diode array. The Raman pump pulse generated as detailed in Ref. [28] exhibited an energy of 1.6 μJ and a focal diameter of 100 μm. Its spectral width which is roughly equivalent to the spectral resolution of the FSRS spectra was determined to be 25 cm^{-1}. The temporal resolution in both types of experiments was around 200 fs. The polarization planes of pump and probe light fields were set to the magic angle. For the TA experiments sample solutions of oNBAc in acetonitrile (Sigma–Aldrich, spectrophotometric grade) of a concentration of 18 mM were employed. For the FSRS experiments perdeuterated acetonitrile (Merck, Uvasol) was used and the concentration adjusted to 10 mM. For the determination of the quantum yield of the *aci*-nitro form THF (Merck, Uvasol) served as a solvent. Sample volumes were around 5 ml and were sufficiently high to render contributions of nitroso photoproducts accumulated during the femtosecond experiment negligible. The solutions were either pumped through a wire guided jet [28,29] (TA, estimated optical pathlength of 150 μm) or a fused silica flow cell (FSRS, pathlength of 500 μm) at a rate high enough to exchange the sample between consecutive laser shots. All experiments were performed at room temperature (22 °C).

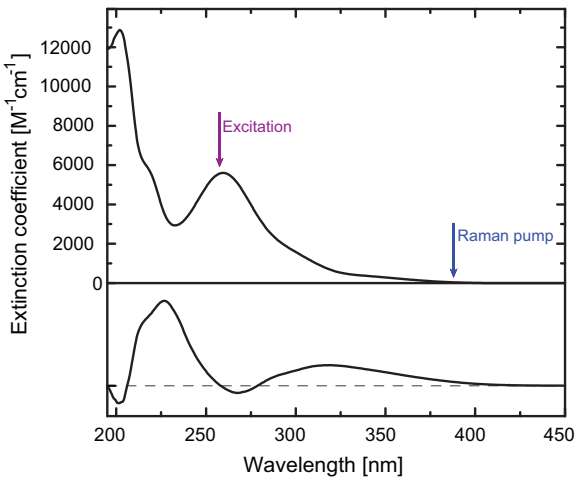

Fig. 1. Absorption spectrum of oNBAc in MeCN (upper panel) and difference spectrum resulting from the 360 nm illumination of a NBAc solution. Arrows mark the wavelengths for the excitation and the Raman pump in the femtosecond experiments.

oNBAc was synthesized by treating *ortho*-nitrobenzylic alcohol with acetyl chloride by standard methods [30]. The crude product was purified by column chromatography. oNBAc was identified by ^1H NMR, IR-spectroscopy, and its melting point. The melting point obtained was 37 °C matching values reported in Refs. [31,32]. Serafinowski et al. [33] reported a higher value of 53–55 °C which we consider erroneous.

3. Results

The absorption spectrum of oNBAc dissolved in acetonitrile features weak transitions which become discernible for wavelengths smaller than 400 nm and stronger ones that peak around 250 and 200 nm (Fig. 1). Upon continuous wave illumination of a oNBAc solution bands are seen to rise at ~320 and 225 nm at the expense of the oNBAc bands 250 and 200 nm (see difference spectrum in Fig. 1). These spectroscopic changes are indicative for the photo-induced formation of *ortho*-nitrosobenzaldehyde [17]. In the TA experiment the laser excitation was tuned to 258 nm. Absorption changes induced by this excitation were probed in the range of 310–755 nm (Fig. 2). Around time zero an intense transient absorption increasing in height towards smaller wavelengths is observed. Within the instrumental response time (200 fs) this intense absorption gives way to a weaker one characterized by a very broad band around 700 nm, one around 400 nm and one peaking at ~320 nm. On the

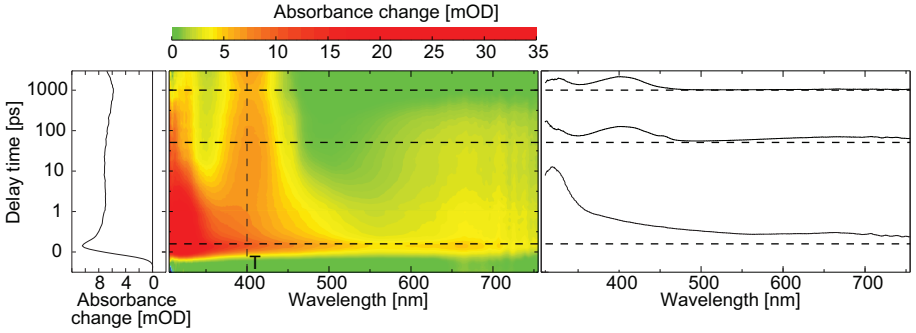

Fig. 2. Transient absorption data of oNBAc dissolved in MeCN. Sample solutions were excited at 258 nm with femtosecond laser pulses. The change in absorption was probed in the range 310–755 nm. In the central contour plot red coloring indicates large positive absorption change, negative ones were not observed. A representative time trace at 400 nm (marked by the dashed line and the **T** in the contour map) is plotted on the left. Note that the time axis is linear until 1 ps and logarithmic thereafter. Transient absorption spectra at 200 fs, 50 ps, and 1 ns are plotted on the right. The dashed horizontal lines correlate these spectra with the contour map. (For interpretation of the references to color in this figure legend, the reader is referred to the web version of this article.)

10 ps time scale these spectral features become "more defined", i.e. the bands narrow. Within some 100 ps the signature around 700 nm decays leaving a band peaking at ~400 nm. At this spectral location an additional rise is seen on the time scale of 1 ns.

To retrieve time constants the data set was fitted globally. The trial function was a sum of decaying exponentials each characterized by a time constant τ_i and wavelength depend amplitudes $\Delta A_i(\lambda)$. The set of amplitudes for one time constant constitute one decay associated spectrum (DAS). By a proper convolution the finite instrumental response time was taken into account (for details see Refs. [34,35]). From the above description of the TA data it is evident that at least one exponential term is required to model the nanosecond rise, one to describe the some 100 ps decay around 700 nm, one to account for the "spectral" sharpening on the 10 ps time scale and finally one to parametrize the ultrafast initial decay. When fitting the data it becomes evident that in addition to these four exponential components another component was required to treat a process with a time constant of ~1 ps. Thus, in total five exponential terms plus an offset were employed. The resulting decay associated spectra are compiled in Fig. 3. The spectrum associated with the time constant $\tau_1 \approx 0.05$ ps (the value is smaller than the instrumental response time and thus subject to a large uncertainty) increases in absorbance towards smaller wavelengths and features the largest signal amplitude. The second spectrum ($\tau_2 = 1$ ps) is similar to the first except for smaller amplitude and a shallow minimum around 420 nm. In the third spectrum ($\tau_3 = 8$ ps) a negative contribution around 400 nm is observed adjacent to which positive features are seen. The fourth spectrum ($\tau_4 = 560$ ps) contains a band at around 400 nm and a very broad one at 700 nm. The fifth spectrum ($\tau_5 = 2000$ ps) finally is essentially an inverted offset spectrum. Assignments for the decay associated spectra will be given in Section 4.

The offset spectrum resembles the transient spectrum recorded 20 ns after photo-excitation by laser flash photolysis (Fig. 4). The spectrum recorded by laser flash photolysis can unequivocally be assigned to the *aci*-nitro tautomer and thereby also the offset spectrum. The amplitude of the offset spectrum holds information on the quantum yield ϕ_a of the *aci*-nitro formation. Using a procedure described earlier [26] we will now estimate this yield. The procedure rests on a comparison between TA data recorded for oNBAc and *ortho*-nitrobenzaldehyde (oNBA). (The quantum yield data were obtained using THF as a solvent. Yet, no significant differences between acetonitrile and THF were observed.) Upon photo-excitation oNBA is known to form a ketene intermediate with a quantum yield ϕ_k of ~0.5 [24]. A part of the ketene population reacts via a "hot channel" so that the effective ketene yield $\phi_{k,e}$ equals 0.25 [35]. TA for oNBAc and oNBA were obtained under identical experimental conditions so that signal magnitudes can be directly compared. The *aci*-nitro form of oNBAc and the ketene intermediate of oNBA both exhibit absorption bands around 400 nm (Fig. 4). Due to the structural similarity between the *aci*-nitro form and the ketene intermediate the oscillator strengths $f_{a,k}$ of these bands are likely to be close to each other. This notion is supported by time dependent DFT computations (B3LYP/TZVP) [26] on the *aci*-nitro form of oNT and the ketene intermediate. The computation afforded oscillator strengths for the *aci*-nitro form of oNT of $f_a = 0.16$ and $f_k = 0.11$ for the ketene. We here assume that the *aci*-nitro forms of oNBAc and oNT exhibit the same oscillator strength f_a. Noting that these two *aci*-nitro forms are structurally closer related than the *aci*-nitro form of oNT and ketene intermediate this seems to be justified. The yield of the *aci*-nitro form ϕ_a is calculated from:

$$\phi_a = \phi_{k,e} \frac{\int \Delta A_a(\lambda)\, d\lambda}{\int \Delta A_k(\lambda)\, d\lambda} \cdot \frac{f_k}{f_a}. \quad (1)$$

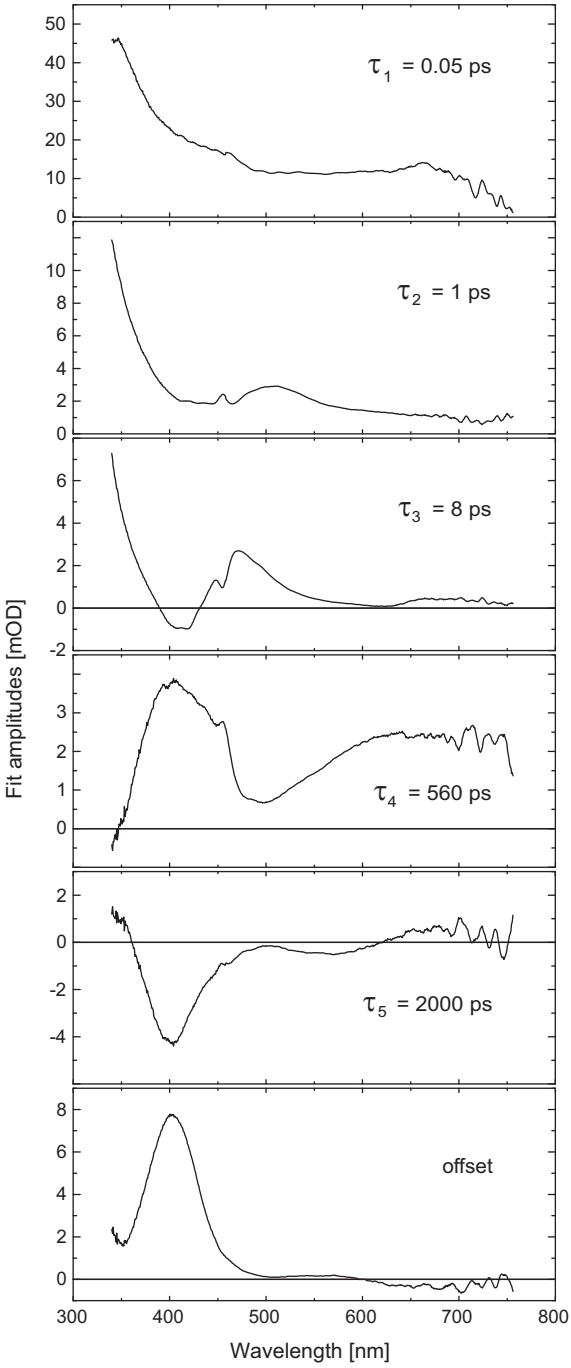

Fig. 3. Decay associated spectra obtained from a global analysis of the transient absorption data depicted in Fig. 2.

The difference spectra $\Delta A_{a,k}(\lambda)$ (a: *aci*-nitro, k: ketene) are the ones depicted in Fig. 4. Since in the relevant region ground state bleach is negligible these difference spectra are identical with the transient spectra of the two intermediates. Integrations over the respective bands were performed since such integrals are proportional to oscillator strengths [36]. The computation affords an *aci*-nitro yield ϕ_a of 0.11 (in THF). This value is very close to the overall photochemical yield ϕ_{ph} of 0.1 [18].

As stated above it is evident that after some nanoseconds the *aci*-nitro form is present. Its formation time is difficult to retrieve from the TA data alone. The spectrum associated with the time constant τ_5 features a negative band exactly at the location of *aci*-nitro absorption. The negative band thus represents a rise of this

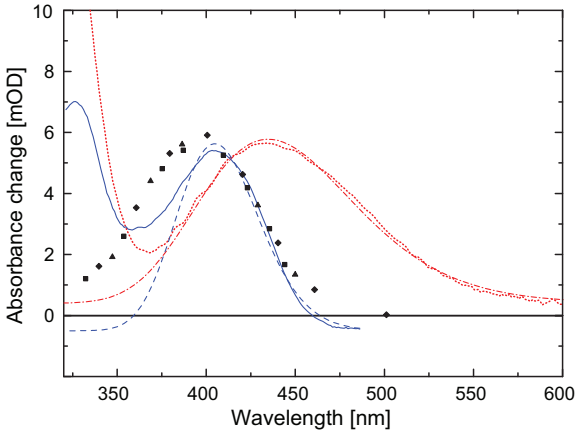

Fig. 4. Comparison of the transient absorption spectrum of oNBAc recorded 3 ns after photo-excitation with the femtosecond apparatus (data: blue, solid line; Gaussian fit: blue, dashed line) with a spectrum recorded after more than 20 ns with a nanosecond set-up (black symbols, data from Ref. [18]) and with the oNBA spectrum after 260 ps (data: red, dotted line; Gaussian fit: red, dash-dotted line) prior to any decay of the ketene absorption. The spectra recorded here were obtained under identical conditions and the signal amplitudes can be compared directly. The spectrum from Ref. [18] has been scaled arbitrarily for comparison. (For interpretation of the references to color in this figure legend, the reader is referred to the web version of this article.)

absorption. Yet, the amplitude of the τ_5 process amounts to only about 50% of the one of the offset spectrum (see Fig. 3). Obviously, a part of the *aci*-nitro population is formed in a faster process. We will now turn to FSRS to obtain information on this faster process. In the FSRS experiment as in the TA measurements a solution of oNBAc in (perdeuterated) acetonitrile was excited at 258 nm with femtosecond laser pulses. The resulting changes of the (stimulated) Raman spectrum were probed using a 388 nm Raman pump pulse. The Raman spectrum of NBAc prior to excitation features pronounced resonances at 1350 and 1575 cm^{-1} due to the symmetric and antisymmetric stretching vibration of the nitro group [37] (Fig. 5).

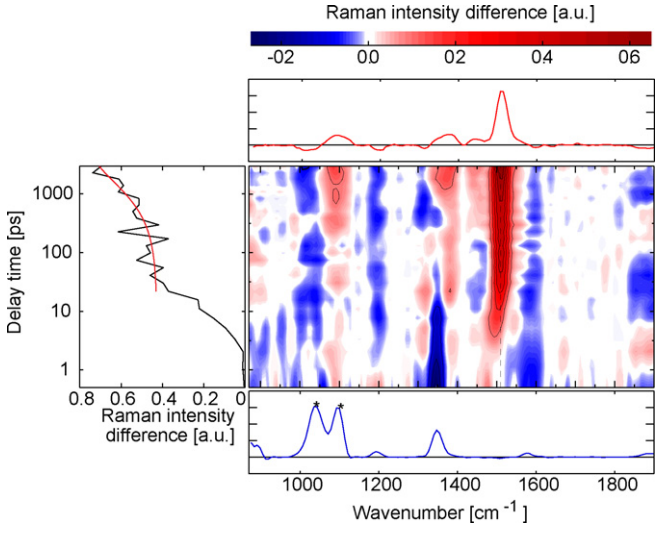

Fig. 5. Femtosecond stimulated Raman data on the photo-reaction of oNBAc in deuterated acetonitrile. As for the transient absorption data the excitation was tuned to 258 nm. Central panel: Contour representation of the FSRS difference data. Red coloring symbolizes positive signals of photoproducts, blue coloring bleaches of the oNBAc starting material. Lower panel: Stationary Raman spectrum of oNBAc. Solvent resonances are marked by a *. Upper panel: Raman difference spectra integrated over the 1–3 ns. On the left a time trace at 1515 cm^{-1} is plotted (black). A fit of the nanosecond rise is plotted in red. (For interpretation of the references to color in this figure legend, the reader is referred to the web version of this article.)

Photo-excitation of oNBAc reduces the ground state population and concomitantly signal bleaches are observed at the spectral positions of the nitro stretching modes and other Raman active modes of NBAc. In addition, positive signals due to transient species show up. We will first describe the spectrum recorded 3 ns after photo-excitation. The spectrum features pronounced resonances at 1370 and 1515 cm^{-1}. The resonance is much higher in intensity than the bleaches. This is due to resonance Raman enhancement. While for ground state oNBAc the Raman pump pulse is pre-resonant (see Fig. 1) it is on resonance with the transient absorption recorded after 3 ns (see Fig. 4). The spectrum is very similar to the one recorded for oNT [26]. Based on time dependent DFT computation that spectrum was assigned to the *aci*-nitro tautomer of oNT. These computations show that the most intense resonance at 1515 cm^{-1} is due to an in-phase ethylenic stretching motion of the two double bonds in the six-membered ring. This motif is of course highly characteristic for *aci*-nitro tautomers. The signal caused by this mode is present well before a couple of nanoseconds. In fact it is clearly discernible 10 ps after photo-excitation and the data suggest that it is already present after 1 ps though peaking at a somewhat lower wavenumber. A time trace in this wavenumber range clearly demonstrates a bi-phasic rise of the *aci*-nitro tautomer (Fig. 5). The characteristic time for the first phase is ~10 ps (as to relevance of this value, see Section 4). Fitting the second rise with a single exponential affords a time constant of 1900 ps and in very good agreement with the value τ_5 = 2000 ps obtained by fitting the TA data.

4. Discussion

The spectroscopic and temporal characteristics described here for photo-reactive oNBAc are very similar to the ones seen for oNT [26] which undergoes a reversible photo-tautomerisation. Thus, it is justified to assign the same processes to these characteristics (cf. Fig. 6): Photo-excitation by 258 nm light promotes NBAc to an upper singlet state. According to time dependent DFT computations [26] for oNT and coupled cluster computations for oNBAc [38] this state is of $\pi\pi^*$ character. Its decay within $\tau_1 \approx 0.05$ ps results in a large decrease of the transient absorption parametrized by the DAS ΔA_1. The decay of the $\pi\pi^*$ state feeds a lower excited state presumably a singlet $n\pi^*$ state. The presence of lower lying $n\pi^*$ states is backed by spectroscopy (see Fig. 1) and quantum chemistry [26,38]. That state in turn decays with a time constant of τ_2 = 1 ps. The respective DAS ΔA_2 exhibits a minimum around 400 nm. This minimum can be regarded as an indicator for the *aci*-nitro formation and/or triplet population. A rise of its 400 nm absorption band would cause a negative contribution in the DAS. Provided that the positive contribution of the decaying $n\pi^*$ state were stronger one obtains as a sum the observed DAS. Further support that the τ_2-decay goes along with the formation of *aci*-nitro form comes from the FSRS data (Fig. 5). The Raman band around 1500 cm^{-1} characteristic for the *aci*-nitro form is first discernible 1 ps after photo-excitation. On the time scale of 10 ps the band shifts to higher wavenumbers and increases in intensity. A shift to higher wavenumbers of vibrational modes is characteristic for vibrational cooling [39,40]. Thus, the time constant τ_3 = 8 ps is assigned to the vibrational cooling of the nascent *aci*-nitro form (concerning the exponential description of a cooling process see Ref. [41]). Time scale and the spectral shape of the DAS ΔA_3 are in accordance with this notion [42]. The DAS ΔA_4 marking the spectral changes caused by the process with the time constant τ_4 = 560 ps exhibits a band at 400 nm and a very broad one around 700 nm. The spectral features and the time constant match the ones of non-reactive nitrobenzenes [19]. The spectral changes are presumably caused by the *decay* of a triplet state. Our TA data do not allow to pinpoint the *rise* of the triplet state since no DAS features a negative

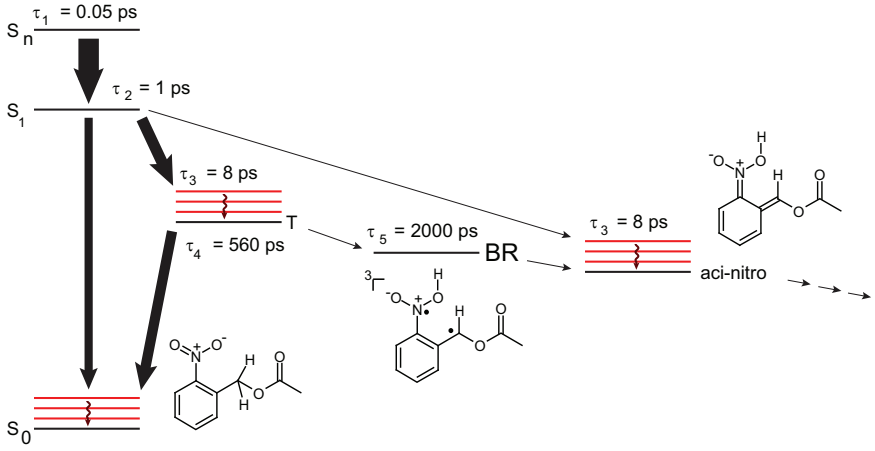

Fig. 6. Kinetic scheme of the photo-reaction of oNBAc. The time constants mark lifetimes of the respective species except for τ_3 which represent a cooling process. The thickness of the arrows represent ratios of rate constants as far applicable.

contribution around 700 nm. So it can only be safely stated that the population of the triplet state occurs during one of the processes τ_1–τ_3. Since the τ_3 process has been assigned to vibrational cooling, population of the triplet state, i.e. intersystem crossing, most likely takes place during the processes τ_1 and τ_2, thereby competing with the internal conversion and/or the *aci*-nitro formation. The slowest process in the temporal window covered features a time constant τ_5 = 2000 ps. The respective DAS ΔA_5 shows that this process goes along with an additional rise of the *aci*-nitro tautomer. This additional rise is perfectly mirrored in the FSRS data. As detailed in Ref. [26] it might be caused by *aci*-nitro tautomers formed via a triplet channel. In the triplet state of oNBAc a hydrogen atom is transferred thereby generating a triplet-phased biradical (see Fig. 6). In this picture the recombination of the biradical occurs with the time constant τ_5.

The spectrum recorded after termination of the τ_5 process resembles the one recorded by flash photolysis (see Fig. 4). In particular the low frequency parts and the maxima match. For the high frequency parts deviations are observed. The spectrum reported here falls off more rapidly than the flash photolysis one. This could be due to systematic errors in one of the measurements or due to a kinetics process occurring with ~10 ns. The *aci*-nitro species might for instance undergo a proton transfer within the protonated nitro-group. Indications for such a process have been observed for oNT, albeit no time constant was determined [26]. Notwithstanding, the signal recorded after 3 ns stems from a *aci*-nitro species. Its signal corresponds to a quantum yield ϕ_a of 0.11. This value is equal to the "overall" deprotection yield [18]. In other words, once formed the *aci*-nitro tautomers release the acetate with a yield of one. Inspection of the DAS ΔA_5 and ΔA_{offset} shows that the fast (singlet, s) and the slow (triplet, t) phase contribute equally to the *aci*-nitro formation, i.e. $\phi_a^s = \phi_a^t = 0.05$. This finding is underscored by the FSRS measurements. For the 1515 cm^{-1} time trace the amplitudes of the slow and the fast rise are nearly equal (0.54 vs 0.46). The yield ϕ_a^t is much smaller than common triplet yields ϕ_t of nitrobenzenes which are of the order of 0.8 [43,44]. Thus, the triplet state of NBAc mostly decays non-reactively and only a small fraction ϕ_a^t forms the biradical. In line with that the triplet lifetime τ_4 is very similar to values reported for non-reactive nitrobenzenes [19,44]. Our findings clearly show that singlet excitation of nitrobenzenes exhibit a much larger photo-reactivity than triplet excitations. The quantum yields $\phi_a^{s,t}$ can be related to

$$\phi_a^{s,t} = \frac{k_r^{s,t}}{k_r^{s,t} + k_{nr}^{s,t}} = k_r^{s,t} \cdot \tau^{s,t}. \quad (2)$$

In the denominator reactive k_r and non-radiative (and non-reactive) rate constants are added. The inverse of this sum equals the lifetime of the singlet and triplet excitation. The singlet lifetime τ^s equals approximately τ_2 = 1 ps and the triplet lifetime τ^t equals τ_4 = 560 ps. Since the quantum yields $\phi_a^{s,t}$ have the same value the reactive rate k_r^s of the singlet state is by a factor of 500 higher than the one of the triplet state.

5. Conclusions

The present study has shown that up to some nanoseconds the photo-reactive oNBAc exhibits kinetics very similar to one of the photo-reversible oNT. In either molecule UV-excitation triggers a hydrogen transfer yielding an *aci*-nitro tautomer. That tautomer is formed via a singlet and a triplet channel. The triplet state has proven to be less reactive than the singlet state by roughly three orders of magnitude. For oNBAc the yield of the *aci*-nitro form equals the one of the overall photo-reaction. Thus, approaches to increase de-caging yields ought to render the initial hydrogen transfer more efficient.

Acknowledgments

This study was supported by the Deutsche Forschungsgemeinschaft via the projects GI349/1-2 and SFB 663, B6.

References

[1] J.A. Barltrop, P. Schofield, Tetrahedron Lett. 16 (1962) 697.
[2] J.A. Barltrop, P.J. Plant, P. Schofield, Chem. Commun. 22 (1966) 822.
[3] W. Patchornik, B. Amit, R.B. Woodward, J. Am. Chem. Soc. 92 (1970) 6333.
[4] A.P. Pelliccioli, J. Wirz, Photochem. Photobiol. Sci. 1 (2002) 441.
[5] J. Engels, E.J. Schlaeger, J. Med. Chem. 20 (1977) 907.
[6] J.H. Kaplan, B. Forbush, J.F. Hoffman, Biochemistry 17 (1978) 1929.
[7] J.A. McCray, D.R. Trentham, Annu. Rev. Biophys. Biophys. Chem. 18 (1989) 239.
[8] G.C.R. Ellis-Davies, Nat. Methods 4 (2007) 619.
[9] A.C. Pease, D. Solas, E.J. Sullivan, M.T. Cronin, C.P. Holmes, S.P.A. Fodor, Proc. Natl. Acad. Sci. U. S. A. 91 (1994) 5022.
[10] M.C. Pirrung, Angew. Chem.-Int. Ed. 41 (2002) 1277.
[11] X.L. Gao, E. Gulari, X.C. Zhou, Biopolymers 73 (2004) 579.
[12] T. Milburn, N. Matsubara, A.P. Billington, J.B. Udgaonkar, J.W. Walker, B.K. Carpenter, W.W. Webb, J. Marque, W. Denk, J.A. McCray, G.P. Hess, Biochemistry 28 (1989) 49.
[13] K. Schaper, S.A.M. Mobarekeh, C. Grewer, Eur. J. Org. Chem. (2002) 1037.
[14] A. Hasan, K.P. Stengele, H. Giegrich, P. Cornwell, K.R. Isham, R.A. Sachleben, W. Pfleiderer, R.S. Foote, Tetrahedron 53 (1997) 4247.
[15] D. Wöll, J. Smirnova, M. Galetskaya, T. Prykota, J. Buhler, K.P. Stengele, W. Pfleiderer, U.E. Steiner, Chem.-Eur. J. 14 (2008) 6490.
[16] J.E.T. Corrie, A. Barth, V.R.N. Munasinghe, D.R. Trentham, M.C. Hutter, J. Am. Chem. Soc. 125 (2003) 8546.
[17] Y.V. Il'ichev, M.A. Schwörer, J. Wirz, J. Am. Chem. Soc. 126 (2004) 4581.

[18] F. Bley, K. Schaper, H. Görner, Photochem. Photobiol. 84 (2008) 162.
[19] R.W. Yip, D.K. Sharma, R. Giasson, D. Gravel, J. Phys. Chem. 88 (1984) 5770.
[20] R.W. Yip, D.K. Sharma, R. Giasson, D. Gravel, J. Phys. Chem. 89 (1985) 5328.
[21] D. Gravel, R. Giasson, D. Blanchet, R.W. Yip, D.K. Sharma, Can. J. Chem.-Rev. Can. Chim. 69 (1991) 1193.
[22] R.W. Yip, Y.X. Wen, D. Gravel, R. Giasson, D.K. Sharma, J. Phys. Chem. 95 (1991) 6078.
[23] G. Wettermark, Nature 194 (1962) 677.
[24] S. Laimgruber, W.J. Schreier, T. Schrader, F. Koller, W. Zinth, P. Gilch, Angew. Chem.-Int. Ed. 44 (2005) 7901.
[25] S. Laimgruber, T. Schmierer, P. Gilch, K. Kiewisch, J. Neugebauer, Phys. Chem. Chem. Phys. 10 (2008) 3872.
[26] T. Schmierer, S. Laimgruber, K. Haiser, K. Kiewisch, J. Neugebauer, P. Gilch, Phys. Chem. Chem. Phys. 12 (2010) 15653.
[27] P. Kukura, D.W. McCamant, R.A. Mathies, Annu. Rev. Phys. Chem. 58 (2007) 461.
[28] S. Laimgruber, H. Schachenmayr, B. Schmidt, W. Zinth, P. Gilch, Appl. Phys. B—Lasers Opt. 85 (2006) 557.
[29] M.J. Tauber, R.A. Mathies, X.Y. Chen, S.E. Bradforth, Rev. Sci. Instrum. 74 (2003) 4958.
[30] T.S. Wheeler, R.L. Shriner, D.A. Scott, Org. Synth. 32 (1952) 72.
[31] C. Paal, A. Bodewig, Ber. 25 (1892) 2961.
[32] M. Wakselman, I. Cerutti, C. Chany, Eur. J. Med. Chem. 25 (1990) 519.
[33] P.J. Serafinowski, P.B. Garland, J. Am. Chem. Soc. 125 (2003) 962.
[34] H. Satzger, W. Zinth, Chem. Phys. 295 (2003) 287.
[35] T. Schmierer, W.J. Schreier, F.O. Koller, T.E. Schrader, P. Gilch, Phys. Chem. Chem. Phys. 11 (2009) 11596.
[36] I.B. Berlman (Ed.), Handbook of Fluorescence Spectra of Aromatic Molecules, second edition, Academic Press, New York/London, 1971.
[37] B. Schrader (Ed.), Infrared and Raman Spectroscopy, VCH, Weinheim/New York/Basel/Cambridge/Tokyo, 1995.
[38] K. Schaper, M. Etinski, T. Fleig, Photochem. Photobiol. 85 (2009) 1075.
[39] P. Hamm, S.M. Ohline, W. Zinth, J. Chem. Phys. 106 (1997) 519.
[40] T. Schrader, A. Sieg, F. Koller, W. Schreier, Q. An, W. Zinth, P. Gilch, Chem. Phys. Lett. 392 (2004) 358.
[41] F.O. Koller, C. Sobotta, T.E. Schrader, T. Cordes, W.J. Schreier, A. Sieg, P. Gilch, Chem. Phys. 341 (2007) 258.
[42] S.A. Kovalenko, S. Schanz, H. Hennig, N.P. Ernsting, J. Chem. Phys. 115 (2001) 3256.
[43] R. Hurley, A.C. Testa, J. Am. Chem. Soc. 90 (1968) 1949.
[44] M. Takezaki, N. Hirota, M. Terazima, J. Phys. Chem. A 101 (1997) 3443.